Optimal control of filamentation in air

Roland Ackermann, Estelle Salmon, Noëlle Lascoux, and Jérôme Kasparian[a)]
Téramobile, LASIM UMR CNRS 5579, Université Lyon 1, 43 Bd du 11 Novembre 1918, F-69622 Villeurbanne Cedex, France

Philipp Rohwetter, Kamil Stelmaszczyk, Shaohui Li, Albrecht Lindinger, and Ludger Wöste
Téramobile, Institut für Experimentalphysik, FU Berlin, Arnimalle 14, D-14195 Berlin, Germany

Pierre Béjot, Luigi Bonacina, and Jean-Pierre Wolf
GAP, Université de Genève, 20 Rue de l'École de Médecine, CH 1211 Genève, Switzerland

(Received 4 July 2006; accepted 5 September 2006; published online 27 October 2006)

The authors demonstrate optimal control of the propagation of ultrashort, ultraintense (multiterawatt) laser pulses in air over distances up to 36 m in a closed-loop scheme. They optimized three spectral ranges within the white-light continuum as well as the ionization efficiency. Optimization results in signal enhancements by typical factors of 2 and 1.4 for the target parameters. The optimization results in shorter pulses by reducing their chirp in the case of white-light continuum generation, while they correct the pulse from its defects and set the filamentation onset near the detector as far as air ionization is concerned. © *2006 American Institute of Physics*. [DOI: 10.1063/1.2363941]

When propagating in air, high-power ultrashort laser pulses undergo filamentation.[1] Filaments result from a dynamic balance between Kerr-lens focusing and defocusing by self-induced plasma generation. In the atmosphere, filaments have been observed up to a few kilometers away from the laser source.[2] They can be generated and propagated even in perturbed conditions such as clouds[3] or turbulence.[4] Their ability to generate a "white-light laser"[5] by self-phase modulation (SPM) as well as long conducting plasma channels opens the way to atmospheric applications.[6]

The possibility of controlling to a certain extent the basic features of the propagation of ultrashort laser pulses has been demonstrated recently. Besides the long-known effect of an initial focusing of the beam,[7] the effects of the initial pulse chirp,[2,8–11] spatial filtering,[12] beam profile,[13] pulse energy,[14] initial focus,[15] and polarization[16] have been investigated. However, since numerical simulation of the propagation of high-power, large-diameter laser pulses is time consuming, it is generally not possible to define the best laser conditions to optimize a specific property of the filaments. The advent of spatial light modulators (SLMs) and acousto-optical modulators made a target optimization of ultrashort laser pulses possible by addressing their spectral components independently, applying specific phase shifts or modulating their intensities. This ability was applied for coherent control of atomic and molecular interactions.[17,18] Since the large number of parameters at play in such optimization prevents in most cases any explicit calculation of the optimal pulse shape, nondeterministic algorithms such as genetic algorithms are widely used to maximize or minimize a predefined experimental parameter.[19] In return, the optimal shape found by the algorithm is often considered to bear information about the physical process at play.[20]

The spectral amplitude and phase dependence of the pulse is expected to affect the filamentation process via different mechanisms.

(1) The envelope intensity profile determines the nonlinear focusing process of the beam.
(2) Propagation in air induces group velocity dispersion, which can be precompensated by spectral phase control.
(3) SPM originates from the intensity variations within the laser pulse envelope. A shaped pulse with steeper intensity fronts will therefore experience a more efficient energy conversion into the white-light continuum.
(4) Multiphoton ionization of air molecules is sensitive to the spectral and temporal pulse characteristics; hence the control of these parameters may result in a change in the dynamic balance between Kerr effect and plasma defocusing, affecting the filamentation process itself.
(5) Retarded Kerr effect might also play a role in the optimal pulse shape.

Notice, moreover, that pulse shaping and closed-loop optimization could also be used to improve the selectivity of multiphoton-excited fluorescence lidar for bioaerosol detection[21] or remote laser induced breakdown spectroscopy[22,23] in the future.

Recently, the use of closed-loop optimization to set the position of filaments in dye-doped water[24] or the yield of second-harmonic generation[25] was reported. In this letter, we demonstrate the optimal control of the propagation of ultrashort, ultraintense (multiterawatt) laser pulses in air over distances up to 36 m. We independently optimized three spectral regions within the white-light continuum as well as the ionization efficiency. We show that the optimized pulse shapes retrieved after the optical and the air-ionization measurements bear the signatures of the different physical mechanisms at the basis of the two processes.

The experiments were performed using the *Teramobile* laser,[8] which delivered 150 fs pulses of 210 mJ centered around 785 nm at a repetition rate of 10 Hz. Light from the supercontinnum was scattered on a neutral diffusive screen located 36 m away from the laser and focused onto a photomultiplier by a 20 cm telescope installed close to the laser in a lidar configuration. The signal in three different spectral bands (360±5, 400±5, and 500±5 nm) was the optimizing

[a)]Electronic mail: jkaspari@lasim.univ-lyon1.fr

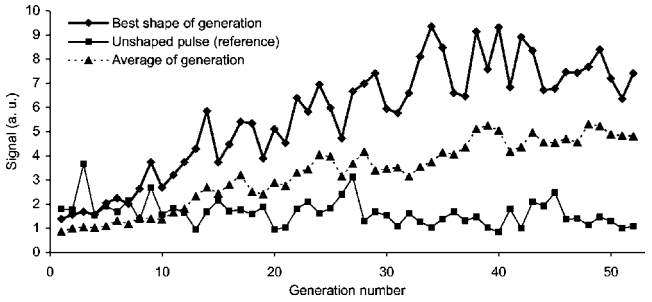

FIG. 1. Typical optimization of the white-light continuum, in the 355–365 nm spectral region.

variable in the optical experiments. Alternatively, optimizations were performed on the electron density, recorded by sonometric measurements[26,27] after 28 m propagation of the laser beam. In both experiments, the signal was averaged over 50 shots.

Closed-loop optimizations[19] were performed using a genetic algorithm[28] and a liquid crystal SLM (2×128 pixels, CRI) placed in the Fourier plane of an afocal 4-f setup.[29,30] The SLM provides a high-resolution spectral shaping of the pulse, but its intrinsic low damage threshold imposed to set it between the stretcher and the regenerative amplifier of the chirped pulse amplification (CPA) laser chain. In this configuration, the amplification distorts the pulse shape applied to the SLM. However, this does not prevent the optimization, since the closed-loop algorithm suppresses the need for an explicit knowledge of the pulse behavior after it leaves the pulse shaper. Instead, the pulse distortions imposed by the amplification are part of the system to optimize. The pulse shaper was used exclusively to control the spectral phase, allowing maximal transmission of the light on each pixel. To reduce the search space, neighboring pixels were binned in sets of 4 , resulting in 32 effective pixels. At each generation, 30 individuals were investigated. To correct for possible drifts of the laser or the atmosphere along the optimization process, a reference signal (unshaped pulse) was recorded at the end of each generation.

Convergence to an optimum pulse shape was achieved after typically 40–60 generations and resulted in an increase in the signal compared to that generated by the reference pulse, for all optimizations performed. The enhancement factor was typically 2 (with a single event yielding a factor of 5) for white light and 1.4 for ionization. As shown in Fig. 1, in the case of the white-light continuum, convergence is achieved in spite of very significant variations of the reference signal over time, showing that the genetic algorithm is able to learn even in a noisy environment. Here, the noise is mainly due to the fluctuations of the 10 Hz laser system, although drifts in the atmosphere also play a role. We checked that repeated optimizations of the same parameter yield comparable results.

Optimizing the white-light continuum (e.g., at 360 nm) from a slightly chirped pulse mainly results in a quadratic phase partly correcting this chirp [see dotted lines in Figs. 2(a) and 2(b)] at the output port of the laser. The chirp is characterized by the slope of the pulse ridge in the time-frequency plane of the Wigner plot. The larger slope of this ridge in the optimized pulse, corresponding to a faster sweep of the wavelengths within the pulse, is the signature for a shorter, less chirped pulse. However, the optimization does not only correct a chirp but instead yields a rich pulse shape [Fig. 2(b)], which was observed to yield up to 20% more signal than could be obtained by tuning the grating compressor to optimize the chirp correction.[8] Maximizations of the white light at all wavelengths considered yield similar phase masks (i.e., the same optimal pulses), resulting in comparable relative signals at different wavelengths and similar spectra of the continuum around the fundamental (between 600 and 900 nm). This latter observation is unexpected, since different pulse shapes would result in different intensity gradient within the pulse envelope and hence in different broadening by SPM. The fact that similar pulse shapes maximize both the generation of the 400 nm and other wavelengths within the continuum indicates that all wavelengths are generated by SPM, while any possible contribution from second-harmonic generation (SHG) to the signal at 400 nm is negligible, even on the surface of the screen, where inversion symmetry is broken so that SHG is not forbidden. Note that our result contrasts with that obtained in the bulk, where, e.g., Schumacher[31] demonstrated the independent optimization of different wavelengths within the supercontinuum. The difference stems from the fact that filamentation is a much more complex process than only SPM in bulk media, as it invokes stabilization of different nonlinear effects such as plasma generation.

In contrast to the optimization of the white-light generation, the optimized pulse for ionization is stretched compared to the initial pulse [Figs. 2(c) and 2(d)], resulting in a longer pulse (800 fs instead of 150 fs typically), as can be seen from the broader extent of the pulse along the temporal axis in the optimized pulse [Fig. 2(d)]. The resulting lower peak power pushes the filament onset away from the laser output. As shown in Fig. 3, the number of filaments increases steeply at the location of the microphone, which is consistent with our previous observation that the sound is maximal at the beginning of the filaments.[26] In other words, the genetic

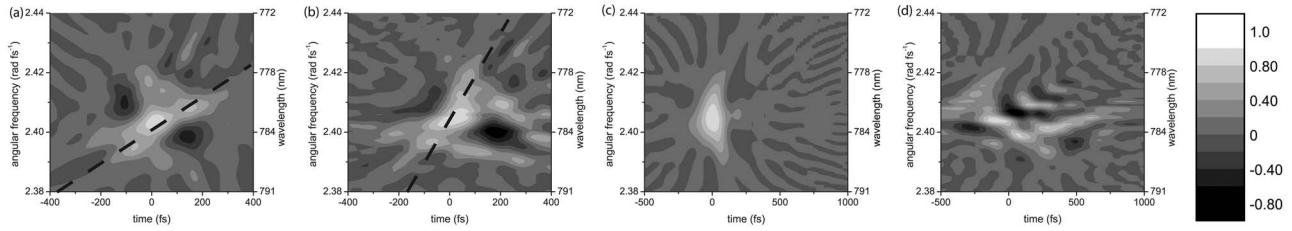

FIG. 2. Normalized Wigner plot of the pulse before (a) and after (b) maximization of the white light at 360 nm, and before (c) and after (d) maximization of the electron density in the filaments. Initial pulses are retrieved from SHG-FROG measurements, while optimized pulses are retrieved from the initial pulses by simulating the geometry of the pulse shaper. Panels (a) and (c) differ because of day-to-day laser fluctuations. The gray scale given on the left is common to all plots.

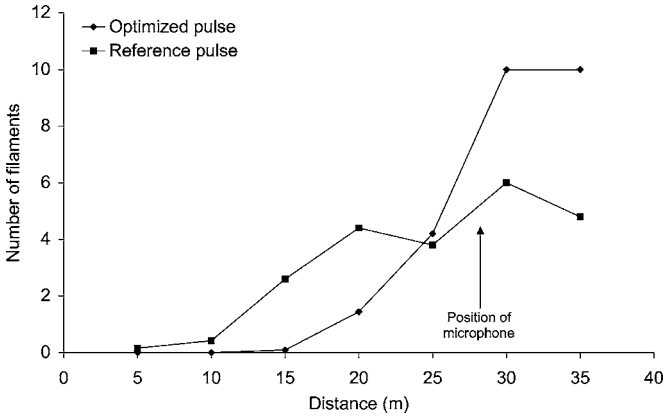

FIG. 3. Filament number as a function of the propagation distance, after optimization for the plasma density and for an unshaped pulse.

algorithm maximizes the plasma generation by maximizing the number of filaments at the location of the detector and setting their onset in this region. Indeed, the filament number increases by a factor of 1.7, close to the factor of 1.4 observed for the ionization signal. This is accomplished essentially by adjusting the chirp and correcting for the discrepancies from a Fourier-transform limited pulse. Moreover, further coherent control enhancing the multiphoton ionization of the air at the onset of the filaments may stem from the complex structure of the Wigner plot of the optimized pulse [Fig. 2(d)]. The change in the filament onset is consistent with the positions observed for chirped pulse of similar duration.[8]

In conclusion, we have demonstrated the optimization of nonlinear processes occurring over long distances in the propagation of multiterawatt laser pulses. Both the generation of visible wavelengths within the white-light continuum and the ionization efficiency at a fixed distance were increased by a factor of 2 and 1.4, respectively, by using optimal control procedures. Although the observed enhancement factor is modest compared to both other results in laboratory conditions and the needs for practical applications, our results demonstrate that pulse shaping can still be performed with high-energy laser pulses, even in relatively unfavorable conditions, including a noisy system and low repetition rate limiting the number of available laser shots per acquisition and hence the number of free parameters.

Nevertheless, the analysis of the optimized shapes shows that optimization of the white-light continuum is achieved by cleaning the pulse shape. Optimizing specific wavelengths within the white-light continuum results in optimizing the whole continuum. On the other hand, optimizing the ionization level at a specific distance mainly results in moving the filamentation onset close to the target location. This finding agrees with the previous observation that electron density decreases along the filament length.[26] Optimizing white-light continuum generation or air ionization within the filaments can be very advantageous for a wide range of applications, including lidar remote sensing, remote light induced breakdown spectroscopy, or the control of high-voltage discharges or lightning.

This work has been performed within the *Teramobile* project, funded jointly by the CNRS, DFG, as well as the French Agence Nationale pour la Recherche under the Grant No. NT05-1_43175. The Teramobile web site is www.teramobile.org.

[1] A. Braun, G. Korn, X. Liu, D. Du, J. Squier, and G. Mourou, Opt. Lett. **20**, 73 (1995).
[2] M. Rodriguez, R. Bourayou, G. Méjean, J. Kasparian, J. Yu, E. Salmon, A. Scholz, B. Stecklum, J. Eislöffel, U. Laux, A. P. Hatzes, R. Sauerbrey, L. Wöste, and J.-P. Wolf, Phys. Rev. E **69**, 036607 (2004).
[3] G. Méjean, J. Kasparian, J. Yu, E. Salmon, S. Frey, J.-P. Wolf, S. Skupin, A. Vinçotte, R. Nuter, S. Champeaux, and L. Bergé, Phys. Rev. E **72**, 026611 (2005).
[4] R. Ackermann, G. Méjean, J. Kasparian, J. Yu, E. Salmon, and J.-P. Wolf, Opt. Lett. **31**, 86 (2006).
[5] S. L. Chin, S. Petit, F. Borne, and K. Miyazaki, Jpn. J. Appl. Phys., Part 2 **38**, L126 (1999).
[6] J. Kasparian, M. Rodriguez, G. Méjean, J. Yu, E. Salmon, H. Wille, R. Bourayou, S. Frey, Y.-B. André, A. Mysyrowicz, R. Sauerbrey, J.-P. Wolf, and L. Wöste, Science **301**, 61 (2003).
[7] E. L. Dawes and J. H. Marburger, Phys. Rev. **179**, 862 (1969).
[8] H. Wille, M. Rodriguez, J. Kasparian, D. Mondelain, J. Yu, A. Mysyrowicz, R. Sauerbrey, J.-P. Wolf, and L. Wöste, Eur. Phys. J.: Appl. Phys. **20**, 183 (2002).
[9] G. Méchain, A. Couairon, Y.-B. André, C. D'amico, M. Franco, B. Prade, S. Tzortzakis, A. Mysyrowicz, and R. Sauerbrey, Appl. Phys. B: Lasers Opt. **79**, 379 (2004).
[10] G. Méchain, C. D'Amico, Y.-B. André, S. Tzortzakis, M. Franco, B. Prade, A. Mysyrowicz, A. Couairon, E. Salmon, and R. Sauerbrey, Opt. Commun. **247**, 171 (2005).
[11] I. S. Golubtsov, V. P. Kandidov, and O. G. Kosareva, Quantum Electron. **33**, 525 (2003).
[12] V. P. Kandidov, N. Akosbek, M. Scarola, O. G. Kosareva, A. V. Nyakk, Q. Luo, S. A. Hosseini, and S. L. Chin, Appl. Phys. B: Lasers Opt. **80**, 267 (2005).
[13] G. Fibich and B. Ilan, J. Opt. Soc. Am. B **17**, 1749 (2000).
[14] G. Méjean, J. Kasparian, J. Yu, E. Salmon, S. Frey, J.-P. Wolf, S. Skupin, A. Vinçotte, R. Nuter, S. Champeaux, and L. Bergé, Phys. Rev. E **72**, 026611 (2005).
[15] S. Skupin, L. Bergé, U. Peschel, F. Lederer, G. Méjean, J. Yu, J. Kasparian, E. Salmon, J. P. Wolf, M. Rodriguez, L. Wöste, R. Bourayou, and R. Sauerbrey, Phys. Rev. E **70**, 046602 (2004).
[16] H. Yang, J. Zhang, Q. Zhang, Z. Hao, Y. Li, Z. Zheng, Z. Wang, Q.-L. Dong, X. Lu, Z. Wei, Z.-M. Sheng, J. Yu, and W. Yu, Opt. Lett. **30**, 534 (2005).
[17] D. Goswami, Phys. Rep. **374**, 385 (2002), and references therein.
[18] M. Dantus and V. V. Lozovoy, Chem. Rev. (Washington, D.C.) **104**, 1813 (2004), and references therein.
[19] R. S. Judson and H. Rabitz, Phys. Rev. Lett. **68**, 1500 (1992).
[20] A. Bartelt, S. Minemoto, C. Lupulescu, S. Vaida, and L. Wöste, Eur. Phys. J. D **16**, 127 (2001).
[21] G. Méjean, J. Kasparian, J. Yu, S. Frey, E. Salmon, and J.-P. Wolf, Appl. Phys. B: Lasers Opt. **78**, 535 (2004).
[22] K. Stelmaszczyk, P. Rohwetter, G. Méjean, J. Yu, E. Salmon, J. Kasparian, R. Ackermann, J.-P. Wolf, and L. Wöste, Appl. Phys. Lett. **85**, 3977 (2004).
[23] M. Y. Shverdin, S. N. Goda, G. Y. Yin, and S. E. Harris, Opt. Lett. **31**, 1331 (2006).
[24] G. Heck, J. Sloss, and R. J. Levis, Opt. Commun. **259**, 216 (2006).
[25] T. Baumert, T. Brixner, V. Seyfried, M. Strehle, and G. Gerber, Appl. Phys. B: Lasers Opt. **65**, 779 (1997).
[26] J. Yu, D. Mondelain, J. Kasparian, E. Salmon, S. Geffroy, C. Favre, V. Boutou, and J. P. Wolf, Appl. Opt. **42**, 7117 (2003).
[27] S. A. Hosseini, J. Yu, Q. Luo, and S. L. Chin, Appl. Phys. B: Lasers Opt. **79**, 519 (2004).
[28] T. Back and H. Schwefel, Evol. Comput. **1**, 1 (1993).
[29] A. M. Weiner, D. E. Leaird, J. S. Patel, and J. R. Wullert, IEEE J. Quantum Electron. **28**, 908 (1992).
[30] S. Vajda, A. Bartelt, C. Kaposta, T. Leisner, C. Lupulescu, S. Minemoto, P. Rosendo-Francisco, and L. Wöste, Chem. Phys. **267**, 231 (2001).
[31] D. Schumacher, Opt. Lett. **27**, 451 (2002).